Check for updates

Batteries & Supercaps

Concept
doi.org/10.1002/batt.202300572

Chemistry Europe
European Chemical Societies Publishing

www.batteries-supercaps.org

Isotope Effects in a Li–S Battery: A New Concept

Xue-Ting Li,[a, b] Yu-Hui Zhu,[a, b] Shuang-Jie Tan,[a] and Sen Xin*[a, b]

Lithium-sulfur battery represents an innovative technology for the next generation electrochemical energy storage, and insight into the fundamentals about its electrochemistry is a key to improved battery storage performance. With years of striving efforts, the interpretation of Li–S reaction mechanism has been extended down to a molecular level. Based on our recent work, we propose to re-examine the Li–S electrochemistry at a (sub)atomic level. Both Li anode and S cathode are made up of mixtures of stable isotopes. Provided with almost the same nucleus structure yet different neutron numbers (and atomic mass), these isotopes could affect the thermodynamic and kinetic parameters of a chemical reaction, and energy storage capability of a Li–S battery. At the cathode, ^{34}S forms stronger S–S bonds and shows higher tendency to react with Li than ^{32}S, so that it helps to improve cathode reaction kinetics. High-order polysulfide anions based on ^{34}S show more sluggish migration in the ether electrolyte than the ^{32}S-based counterparts, which accounts for improved cycling stability of battery. Based on the electrochemical isotope effects of S, a conceptual technology for separating isotopes from natural chalcogen elements was introduced and shows a higher separation factor than the conventional methods.

Introduction

Lithium-sulfur batteries have been intensively studied as high-energy storage devices during the past decades. Taking an advantage from the two-electron Li–S redox reaction, the batteries are expected to offer a theoretical cell-level specific energy of ~2560 Wh/kg and a practical specific energy of $>$600 Wh/kg, making them competitive candidates for powering the next-generation electricity-driven automobiles and aircrafts. The earliest study about Li–S battery can be dated back to the introduction of conceptual S cathode in 1962.[1] During the decades of research, the exploration into mechanism of Li–S reaction has been continuously pushing forward the technological advancement of Li–S battery. Previous studies have shown that,[2] by discharging the S cathode in a liquid (ether) electrolyte, the redox reaction between Li and *cyclo*-octa-S (*cyclo*-S_8) molecules (the most common S allotrope in nature) at the cathode-electrolyte interface undergoes a stepwise fashion. Two plateaus appear in the voltage profile, with the higher voltage at ~2.3 V (vs. Li^+/Li) corresponding to transfer of 0.5 mole of electrons and the lower one at 2.1 V (vs. Li^+/Li) corresponding to transfer of another 1.5 mole of electrons (the number of transferred electrons is calculated based on the cathode reaction, $2Li^+ + 2e^- + S = Li_2S$, where the extend of reaction, $\zeta = 1$ mole). At the first plateau, the *cyclo*-S_8 molecules were reduced to S_4^{2-}, during which high-order polysulfide anions (S_n^{2-}, $4 \leq n \leq 8$) are generated at the cathode-electrolyte (solid-liquid) interface and could be dissolved in the liquid electrolyte. At the second plateau, the high-order lithium polysulfides (LiPSs) are further reduced to insoluble Li_2S_2 and Li_2S.[3–4] The dissolved, high-order LiPSs could diffuse in the electrolyte so that they could even migrate from the cathode to the anode via an electrochemical 'shuttle' process. At the anode surface, a chemical redox reaction occurs between the high-order LiPSs and Li metal, forming a layer of Li_2S_2/Li_2S deposits. The dissolution and shuttle of high-order LiPSs, and the corrosion/passivation of anode surface by non-conductive Li_2S_2/Li_2S pose giant challenges to the stable cycling and capacity retention of Li–S batteries.

To inhibit LiPSs shuttle, many previous strategies have been proposed, which include encapsulation of S particles in nano-sized carbon pores, and use of catalysts to accelerate polysulfides conversion and interlayers that physically block or chemically adsorb the sulfides.[5–10] For these studies, the S cathode consists primarily of bulk S particles or nanosized S aggregates, and fundamentally, the electrochemical reaction between *cyclo*-S_8 and Li is not changed. In 2012, a pioneer study led by Guo et al. proposed to stabilize the Li–S electrochemistry via altering the reaction mechanism at a molecular level.[11] Instead of using a *cyclo*-S_8-based cathode, they prepared, by taking advantages from the space confinement of sub-nano carbon pores, small S_{2-4} allotropes that are directly reduced to insoluble low-order LiPSs. In this way, formation of soluble high-order LiPSs is essentially avoided, and the Li–S batteries show much improved cycling performance.

An (electro)chemical reaction occurs when chemical bonds between atoms are broken and reformed. Acquiring insights into the interatomic interactions is highly important for precisely depicting the reaction mechanism. In this aspect, stable isotopes have offered a good opportunity to picture the reaction at a (sub)atomic level. Stable isotopes refer to a set of

[a] X.-T. Li, Y.-H. Zhu, Dr. S.-J. Tan, Prof. S. Xin
CAS Key Laboratory of Molecular Nanostructure and Nanotechnology,
CAS Research/Education Center for Excellence in Molecular Sciences,
Beijing National Laboratory for Molecular Sciences (BNLMS),
Institute of Chemistry,
Chinese Academy of Sciences (CAS)
Beijing 100190 (P. R. China)
E-mail: xinsen08@iccas.ac.cn

[b] X.-T. Li, Y.-H. Zhu, Prof. S. Xin
University of Chinese Academy of Sciences
Beijing 100049 (P. R. China)

Supporting information for this article is available on the WWW under https://doi.org/10.1002/batt.202300572

© 2024 Wiley-VCH GmbH

non-radioactive atoms occupying the same grid on the Periodic Table. By holding the same number of protons (and electrons) yet different number of neutrons, the isotopes and their compounds usually show similar physicochemical properties. Therefore, isotope substitution does not affect the potential energy surface within Born-Oppenheimer approximation.[12] However, as the isotopes have different nucleus masses, the isotopic substitution does affect the mass-related properties, such as the vibrational frequency and zero-point energy of a molecule, which in turn accounts for different thermodynamic and kinetic parameters of an (electro)chemical reaction (e.g., entropy and free energy change).[13] It has been found in our previous work that aqueous electrolytes based on heavy water (D_2O) show much stronger intermolecular hydrogen bonds than the counterparts based on light water (H_2O), so that the D_2O-based electrolytes are thermodynamically more stable.[14] The thermodynamic effect of stable hydrogen isotopes accounts for a broader electrochemical window and higher anodic stability of D_2O-based electrolytes, and contributes to improved storage performance of aqueous Li–ion batteries. The findings in hydrogen isotope effects inspires us to continue exploring the isotope electrochemistry in a rechargeable Li–S battery.

Stable isotope combinations in a Li–S battery

From the view of isotope chemistry, both the anode and cathode of a Li–S battery are not pure elements. The Li metal consists of ^{6}Li and ^{7}Li (Figure 1a), and the natural S cathode consists of four stable isotopes (^{32}S, ^{33}S, ^{34}S and ^{36}S), in which ^{32}S and ^{34}S hold the largest shares (Figure 1b).[15] If one simply considers natural S as a binary system of ^{32}S/^{34}S, four anode-cathode combinations will be yielded: ^{6}Li–^{32}S, ^{7}Li–^{32}S, ^{6}Li–^{34}S and ^{7}Li–^{34}S (Figure 1c). The theoretical specific energy of the four combinations, as calculated solely based on the electrode active materials (Note S1), is summarized in Figure 1d. It is worth noting that ^{6}Li delivers a theoretical specific capacity of 4467 mAh/g (Note S2), which represents the highest value among the metal electrodes. A ^{6}Li–^{32}S battery with the lightest anode-cathode combination shows the highest theoretical specific energy of 2701 Wh/kg, while a ^{7}Li–^{34}S battery consisting of heavier isotopes shows the lowest value of 2475 Wh/kg. The other two combinations, ^{7}Li–^{32}S (the most common Li–S combination) and ^{6}Li–^{34}S deliver the same theoretical specific energy of 2583 Wh/kg. For practical Li–S batteries, the variation in energy density among different anode-cathode combinations could be insignificant, as both Li and S take up small mass fractions of the full battery. A 10-Ah pouch cell was projected to evaluate the specific energy under practical conditions (Note S3), and the results were summarized in Table S1 and Figure 1e. Benchmarking against the ^{7}Li–^{32}S combination, the other isotope combinations show energy increments from +1.51% for ^{6}Li–^{32}S to −1.29% (^{6}Li–^{34}S) and finally to −2.59% (^{7}Li–^{34}S).

Electrochemical isotope effects of S element

In our recent study, prototype Li–^{32}S and Li–^{34}S batteries were assembled and tested to assess the variation in the electrochemical properties of S isotopes. According to Figures 2a and 2b, the Li–^{34}S battery demonstrates notably reduced voltage polarization, and much higher capacity retention upon cycling than the Li–^{32}S battery. The results indicate that the Li–^{34}S battery shows inhibited LiPSs shuttle and improved cathode reaction kinetics at the solid-liquid interface. Based on our previous study on heavy water,[14] *cyclo*-$^{34}S_8$ could form stronger S–S bonds than *cyclo*-$^{32}S_8$, and show higher tendency to react with Li. In this way, the electrochemical conversion from *cyclo*-S_8 to high-order LiPSs is promoted, which leads to improved reaction kinetics at cathode-electrolyte interface. In this work, molecular dynamics (MD) simulation was performed to study the LiPSs migration in Li–^{32}S and Li–^{34}S batteries. Since Li_2S_6

Xue-Ting Li is a doctoral student at the Institute of Chemistry, CAS (ICCAS). Her research interests focus on the electrochemical isotope effects of chalcogen elements in rechargeable batteries.

Sen Xin received his PhD degree in Physical Chemistry from ICCAS in 2013. He worked with Prof. John B. Goodenough as a postdoctoral fellow at the University of Texas at Austin from 2015 to 2019, and joined ICCAS as a full professor in 2019. His research interests focus on materials and interfacial chemistry, and electrochemical isotope effects in high-energy rechargeable batteries.

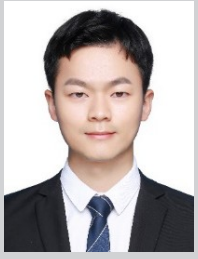

Shuang-Jie Tan received his PhD degree in Materials Science from ICCAS in 2021. From 2021 to 2023, he worked with Prof. Yu-Guo Guo as a postdoctoral fellow at ICCAS. His research interests focus on the high-performance energy storage battery materials, including lithium metal anode and non-flammable electrolytes.

© 2024 Wiley-VCH GmbH

25666223, 2024, 4, Downloaded from https://chemistry-europe.onlinelibrary.wiley.com/doi/10.1002/batt.202300572 by University of Ulsan, Wiley Online Library on [11/11/2025]. See the Terms and Conditions (https://onlinelibrary.wiley.com/terms-and-conditions) on Wiley Online Library for rules of use; OA articles are governed by the applicable Creative Commons License

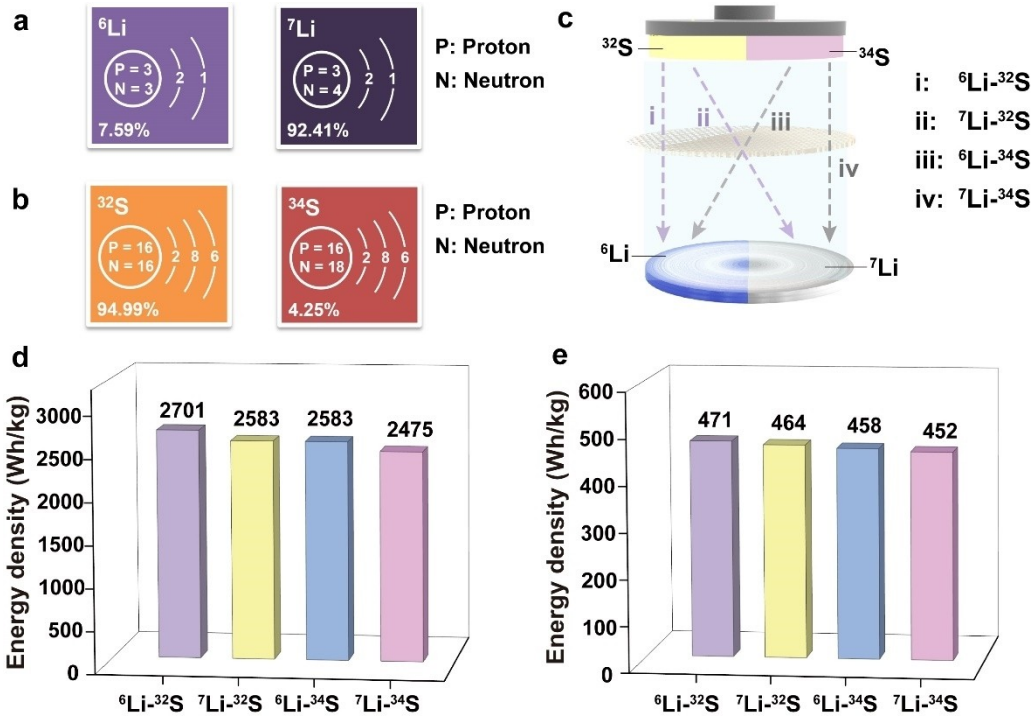

Figure 1. Fundamentals about the objective isotopes in a Li–S battery, which include nucleus structure and abundance (in atomic percentage) of (a) ^{6}Li and ^{7}Li, and (b) ^{32}S and ^{34}S isotopes. (c) A schematic of four isotope combinations, and the theoretical specific energy of the four combinations calculated based on (d) the net mass of Li and S, and (e) the total mass of a 10-Ah pouch cell.

contributes mostly to the LiPSs shuttle, a model system consisting of Li_2S_6, $LiPF_6$ salt and 1,2-dimethoxy ethane (DME) molecules was employed. According to Figure 2c, d and Note S4, $^{34}S_6^{2-}$ shows a lower diffusion coefficient (0.770×10^{-6} cm^2/s) than $^{32}S_6^{2-}$ (1.184×10^{-6} cm^2/s), which agrees with the experimental results and indicates more sluggish migration of polysulfide anions in the Li–^{34}S battery.

Herein, the varied mobility of isotopic LiPS anions in the battery is ascribed to the intimate chemical interactions between the anions and the environment. A "cation-anion-solvent (CAS)" model is proposed to describe the complex interactions between Li^+, S_6^{2-} and solvent (Figure 3a). The Li^+-S_6^{2-} interaction forms the basis of LiPSs shuttle,[16] and it competes against the Li^+-solvent interaction (via Li–O bond). The Li^+-solvent interaction is related with solvation of LiPSs and has a positive effect on cathode reaction kinetics. According to Figures 3b-e, both ^{34}S-based and ^{32}S-based LiPSs show similar solvation structures, yet $^{34}S_6^{2-}$ exhibits stronger cation-solvent interaction and weaker cation-anion interaction than $^{32}S_6^{2-}$. In this way, the ^{34}S cathode shows faster polysulfide conversion at the solid-liquid interface and inhibited dissolution and shuttle of LiPSs in the electrolyte (Figure 3f), which contributes to improved electrochemical performance.

S isotopes separation

Heavy S isotope (^{34}S) seems to be a preferential choice for enabling Li–S cells with improved cycling and rate performance. However, the use of ^{34}S to build a practical Li–S battery is still challenging. Though ^{34}S has a claimable abundance comparable with that of common metal elements, its use as cathode material is still hindered by a high price of $>$1500 USD per gram. The reason lies in a low separation ratio of ^{32}S/^{34}S by using the conventional methods, which leads to a complex separation process that inevitably increases the cost.[17] Taking advantages of the electrochemical isotope effects, we proposed to separate ^{32}S and ^{34}S by simply using a Li–S coin cell. The battery consists of a natural S cathode, a Li–metal anode and a conventional ether electrolyte. Figure 4a shows the depth profiles of $^{32}S^-$ and $^{34}S^-$ obtained by time-of-flight secondary ion mass spectrometry (ToF-SIMS) from the uncycled S cathode. Based on the two profiles, the ^{32}S/^{34}S atomic ratios were calculated and plotted against the sputtering time. By increasing the sputtering time, the value is stabilized at around 22.35 (Figure 4b), which matches well with the ^{32}S/^{34}S ratio of natural S. Figure 4c shows the depth profiles of $^{32}S^-$ and $^{34}S^-$ collected from the Li–metal anode after 10 (dis)charge cycles, which yields a ^{32}S/^{34}S ratio of 26.85-30.80 according to Figure 4d. With the ^{32}S/^{34}S ratios obtained from the uncycled cathode and the cycled anode, a separation factor in the form of δ(‰) is calculated to be 200–370 for the cycled Li–S battery (Note S5). Therefore, by using the Li–S battery (LiS, whose principle of S isotopes separation is described in Figure 4e), the isotope separation factor is increased by at least one or two orders of magnitude, compared with the values obtained using the conventional methods of bacterial metabolism (BM), distillation (Dtl) and chemical exchange (CE) (Figure 4f).

© 2024 Wiley-VCH GmbH

25666223, 2024, 4, Downloaded from https://chemistry-europe.onlinelibrary.wiley.com/doi/10.1002/batt.202300572 by University of Ulsan, Wiley Online Library on [11/11/2025]. See the Terms and Conditions (https://onlinelibrary.wiley.com/terms-and-conditions) on Wiley Online Library for rules of use; OA articles are governed by the applicable Creative Commons License

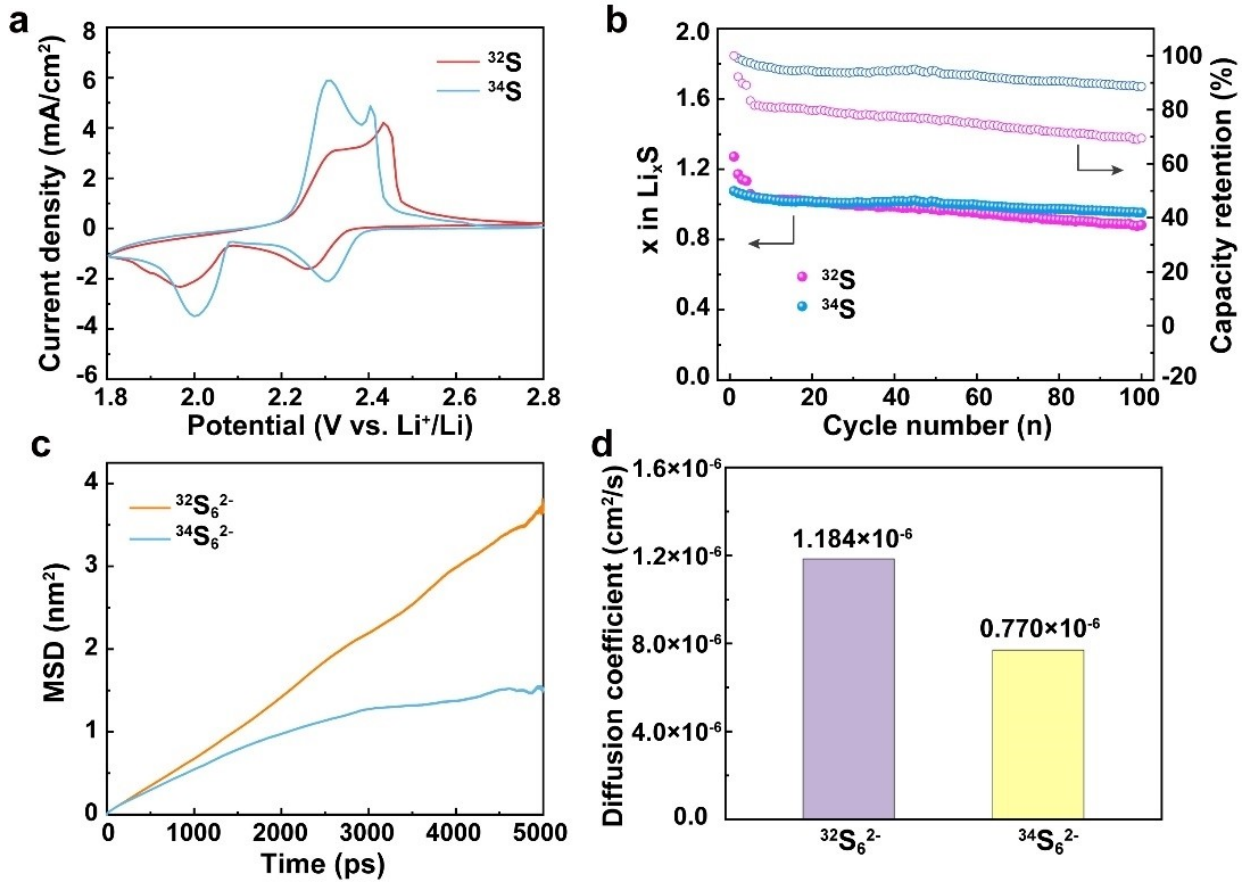

Figure 2. (a) Cyclic voltammetry profiles of the Li–^{32}S and Li–^{34}S cells. (b) Cycling performance and capacity retention of the Li–^{32}S and Li–^{34}S cells for 100 (dis)charge cycles. (c) Mean square displacement (MSD) diagrams of $^{32}S_6^{2-}$ and $^{34}S_6^{2-}$ with time calculated by MD simulation. (d) Calculated diffusion coefficient of $^{32}S_6^{2-}$ and $^{34}S_6^{2-}$ anions.

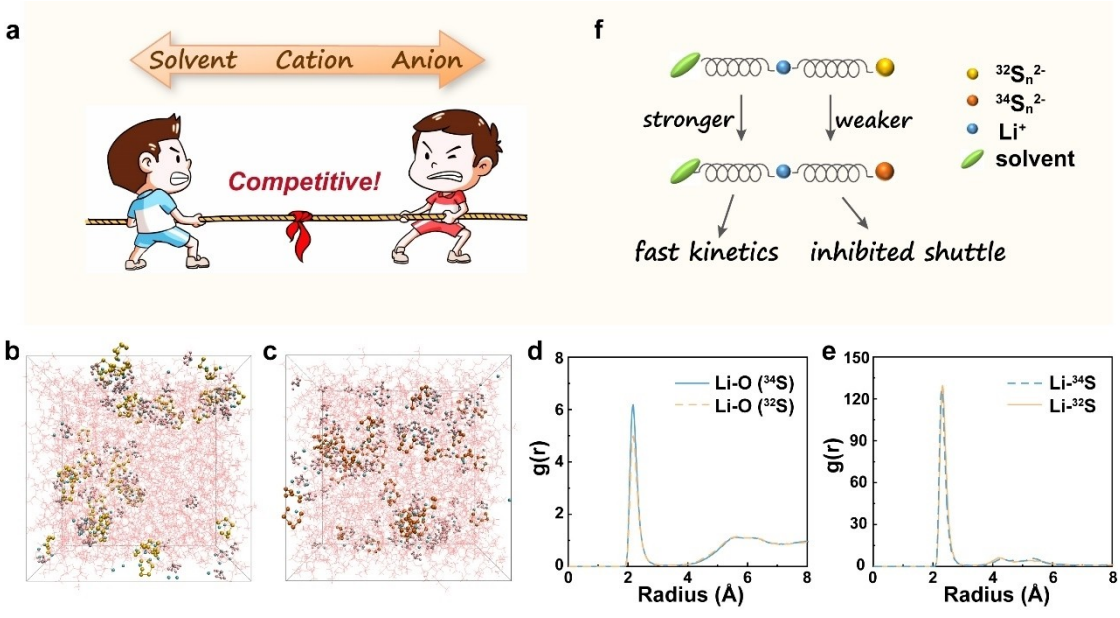

Figure 3. Chemistry of high-order LiPSs in the ether solvent, including, (a) the "CAS" model that describes the cation-anion-solvent interactions in the electrolyte, snapshots showing solvation structures of (b) $Li_2{}^{32}S_6$ in DME and (c) $Li_2{}^{34}S_6$ in DME by MD simulation (Li cations, blue; ^{32}S atoms, yellow; ^{34}S atoms, orange; P atoms, grey; F atoms, pink; DME, pink lines), radical distribution function of (d) Li–O, and (e) Li–S for $Li_2{}^{32}S_6$ and $Li_2{}^{34}S_6$ with DME (Some key parameters for calculation are listed in Table S2) and (f) working mechanism of improving the Li–S electrochemistry by ^{34}S according to the "CAS" model.

© 2024 Wiley-VCH GmbH

25666223, 2024, 4, Downloaded from https://chemistry-europe.onlinelibrary.wiley.com/doi/10.1002/batt.202300572 by University of Ulsan, Wiley Online Library on [11/11/2025]. See the Terms and Conditions (https://onlinelibrary.wiley.com/terms-and-conditions) on Wiley Online Library for rules of use; OA articles are governed by the applicable Creative Commons License

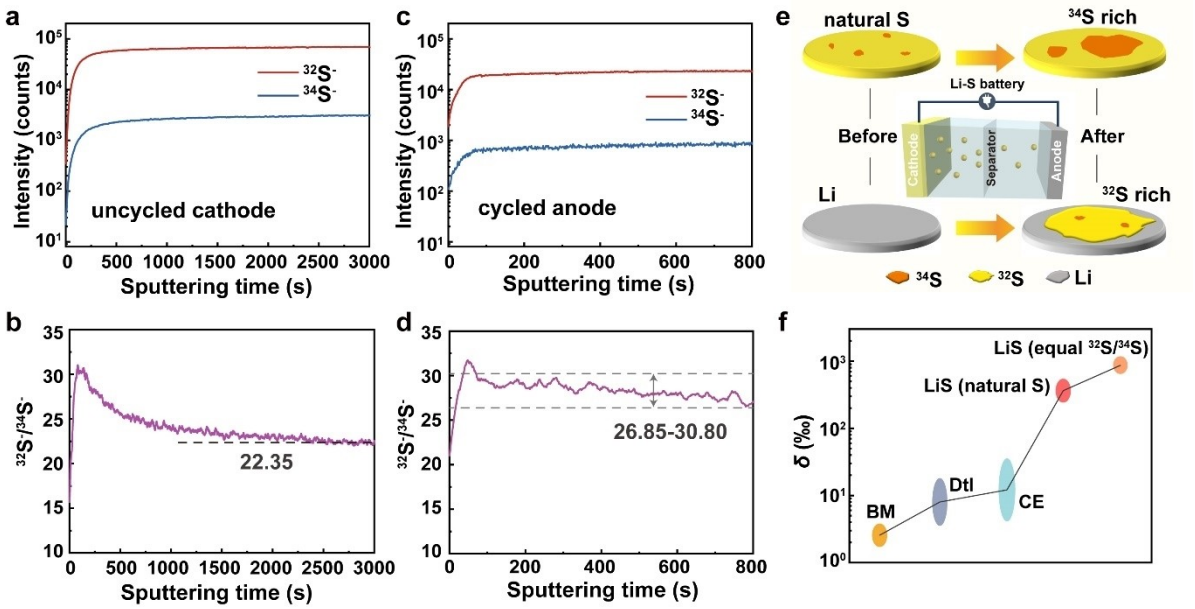

Figure 4. Electrochemical isotope separation of natural S by a Li–S coin cell, including, (a) ToF-SIMS depth profiles of $^{32}S^-$ and $^{34}S^-$ fragments collected from the uncycled natural S cathode, (b) $^{32}S/^{34}S$ atomic ratio calculated from the profiles in (a), (c) ToF-SIMS depth profiles of $^{32}S^-$ and $^{34}S^-$ fragments collected from the cycled Li–metal anode, (d) $^{32}S/^{34}S$ atomic ratio calculated from the profiles in (c), (e) a schematic showing the principle of electrochemical isotope separation, and (f) separation factors in the form of δ(‰) for $^{32}S/^{34}S$ isotopes by different methods.[17]

Recently in our group, a separation factor of 600–1000 was obtained for another Li–S cell employing an equimolar $^{32}S/^{34}S$ mixture (a $^{32}S/^{34}S$ ratio of 1) as the cathode material, which is higher than the value of the present study. By comparing the two studies, it appears that the molar fraction of ^{34}S in the isotope mixture positively affects the separation factor. However, both studies support the conclusion that ^{34}S is enriched at the cathode while ^{32}S is enriched at the anode (Figure 4e).

In addition to ^{32}S and ^{34}S, we have also considered the electrochemical separation and enrichment of other two stable S isotopes (^{33}S: 0.75 atom.%; ^{36}S: 0.01 atom.%).[15] Nevertheless, their SIMS signals collected from the cycled anode almost fall below the lower limit of detection of the instrument (*ca.* 10^{-7} mol/cm^2 for ^{33}S and 10^{-9} mol/cm^2 for ^{36}S), in the case natural S was employed as the cathode material (based on an areal S mass loading of 0.5 mg/cm^2). Hence, even though ^{33}S and ^{36}S show electrochemical isotope effect in a Li–S coin cell, it remains difficult to directly observe the influence on battery performance or isotope separation. Proper battery configurations, such as Ah-level pouch cells, may help to magnify the isotope effects of $^{33}S/^{36}S$.

Summary and Outlook

Scientific research on stable isotopes has lasted for over a century, yet the effects of rare isotopes on the reaction of a rechargeable battery have long been underestimated.[18–19] By unveiling the isotope effects in a Li–S battery, we propose to reevaluate the isotope-based variations in thermodynamic and kinetic parameters of an electrochemical reaction, and more importantly, offer a new perspective on separation of isotopes in a rechargeable battery. Compared with the conventional methods, the new separation technology aims for higher efficiency, lower energy consumption and simpler procedures.[20] In view of the analogous electrochemical properties of chalcogen elements in rechargeable Li batteries,[21] the strategy could be applied to separating selenium (Se) and tellurium (Te) isotopes from their natural elements. Other elements, such as halogens,[22–23] may also take advantage of the electrochemical isotope effects. On a smaller scale, we are prepared to share exciting new stories.

Supporting Information

The authors have cited additional references within the Supporting Information.[24–35]

Acknowledgements

This work was supported by Beijing Natural Science Foundation (Grant Nos. JQ22005 and Z220021), the National Key R&D Program of China (Grant No. 2019YFA0705703), CAS Project for Young Scientists in Basic Research (Grant No. YSBR-058), National Natural Science Foundation of China (Grant Nos. 52172252, 21975266 and 22309187). S.-J. T. acknowledges the China Postdoctoral Science Foundation (Grant 2021 M703268) and the Junior Fellow Program of Beijing National Laboratory for Molecular Sciences (Grant 2021BMS20062). The authors thank Prof. Yao Zhao at ICCAS for performing the ToF-SIMS experiments.

© 2024 Wiley-VCH GmbH

25666223, 2024, 4, Downloaded from https://chemistry-europe.onlinelibrary.wiley.com/doi/10.1002/batt.202300572 by University of Ulsan, Wiley Online Library on [11/11/2025]. See the Terms and Conditions (https://onlinelibrary.wiley.com/terms-and-conditions) on Wiley Online Library for rules of use; OA articles are governed by the applicable Creative Commons License

Conflict of Interests

The authors declare no conflict of interest.

Keywords: stable sulfur isotopes · lithium-sulfur battery · polysulfide shuttle · isotope effect · isotope separation

[1] H. Danuta, U. Juliusz, "Electric dry cells and storage batteries", **1962–07-10**, US3043896 A.
[2] Y.-X. Yin, S. Xin, Y.-G. Guo, L.-J. Wan, *Angew. Chem. Int. Ed.* **2013**, *52*, 13186–13200.
[3] H. Pan, Z.-B. Cheng, Z.-Y. Zhou, S.-J. Xie, W. Zhang, N. Han, W. Guo, J. Fransaer, J. Luo, A. Cabot, M. Wübbenhorst, *Nano-Micro Lett.* **2023**, *15*, 165.
[4] Y. Li, K. K. Fu, C.-J. Chen, W. Luo, T.-T. Gao, S.-M. Xu, J. Dai, G. Pastel, Y.-B. Wang, B.-Y. Liu, J.-W. Song, Y.-N. Chen, C.-P. Yang, L.-B. Hu, *ACS Nano* **2017**, *11*, 4801–4807.
[5] J. Chou, Y.-H. Wang, W.-P. Wang, S. Xin, Y.-G. Guo, *J. Electrochem.* **2023**, *29*, 2217009.
[6] R. Yan, Z.-Y. Zhao, M.-H. Cheng, Z. Yang, C. Cheng, X.-K. Liu, B. Yin, S. Li, *Angew. Chem. Int. Ed.* **2023**, *62*, e202215414.
[7] L. Chen, T. He, K.-X. Liao, H. Lu, J. Ma, Y.-T. Feng, S. Meng, C. Zhang, J.-H. Yang, *Adv. Mater.* **2023**, 2308587.
[8] R. Razaq, M. M. U. Din, D. R. Småbråten, V. Eyupoglu, S. Janakiram, T. O. Sunde, N. Allahgoli, D. Rettenwander, L. Deng, *Adv. Energy Mater.* **2023**, 2302897.
[9] X. Li, J.-D. Liu, J. He, S.-H. Qi, M.-G. Wu, H.-P. Wang, G.-X. Jiang, J.-D. Huang, D.-X. Wu, F. Li, J.-M. Ma, *Adv. Sci.* **2022**, *9*, 2201297.
[10] D.-S. Bin, Y.-S. Xu, S.-J. Guo, Y.-G. Sun, A.-M. Cao, L.-J. Wan, *Acc. Chem. Res.* **2021**, *54*, 221–231.
[11] S. Xin, L. Gu, N.-H. Zhao, Y.-X. Yin, L.-J. Zhou, Y.-G. Guo, L.-J. Wan, *J. Am. Chem. Soc.* **2012**, *134*, 18510–18513.
[12] M. Cardona, M. L. W. Thewalt, *Rev. Mod. Phys.* **2005**, *77*, 1173–1224.
[13] M. Gómez-Gallego, M. A. Sierra, *Chem. Rev.* **2011**, *111*, 4857–4963.
[14] J. Chou, Y. Zhao, X.-T. Li, W.-P. Wang, S.-J. Tan, Y.-H. Wang, J. Zhang, Y.-X. Yin, F.-Y. Wang, S. Xin, Y.-G. Guo, *Angew. Chem. Int. Ed.* **2022**, *61*, e202203137.
[15] E. Roduner, in *Isotope Effects In Chemistry and Biology*, 1st ed. (Eds.: A. Kohen, H.-H. Limbach), CRC Press, Boca Raton, **2005**, pp. 433–448.
[16] E. P. Kamphaus, P. B. Balbuena, *J. Phys. Chem. C* **2017**, *121*, 21105–21117.
[17] M. A. Boris, A. S. Polevoi, *Russ. Chem. Rev.* **1983**, *52*, 213.
[18] J. Y. Kim, H. Oh, H. R. Moon, *Adv. Mater.* **2019**, *31*, 1805293.
[19] B. J. Peterson, B. Fry, *Annu. Rev. Ecol. Syst.* **1987**, *18*, 293–320.
[20] P. A. Sossi, G. P. Halverson, O. Nebel, S. M. Eggins, *Geostand. Geoanal. Res.* **2015**, *39*, 129–149.
[21] J. Xu, J. Ma, Q. Fan, S. Guo, S. Dou, *Adv. Mater.* **2017**, *29*, 1606454.
[22] S. Chen, J.-T. Zhang, *Dalton Trans.* **2020**, *49*, 9929–9934.
[23] Z.-Y. Xue, Z.-Y. Gao, X.-Y. Zhao, *Energy Environ. Mater.* **2022**, *5*, 1155–1179.
[24] M. J. Frisch, G. W. Trucks, H. B. Schlegel, G. E. Scuseria, M. A. Robb, J. R. Cheeseman, G. Scalmani, V. Barone, G. A. Petersson, H. Nakatsuji, X. Li, M. Caricato, A. V. Marenich, J. Bloino, B. G. Janesko, R. Gomperts, B. Mennucci, H. P. Hratchian, J. V. Ortiz, A. F. Izmaylov, J. L. Sonnenberg, Williams, F. Ding, F. Lipparini, F. Egidi, J. Goings, B. Peng, A. Petrone, T. Henderson, D. Ranasinghe, V. G. Zakrzewski, J. Gao, N. Rega, G. Zheng, W. Liang, M. Hada, M. Ehara, K. Toyota, R. Fukuda, J. Hasegawa, M. Ishida, T. Nakajima, Y. Honda, O. Kitao, H. Nakai, T. Vreven, K. Throssell, J. A. Montgomery Jr., J. E. Peralta, F. Ogliaro, M. J. Bearpark, J. J. Heyd, E. N. Brothers, K. N. Kudin, V. N. Staroverov, T. A. Keith, R. Kobayashi, J. Normand, K. Raghavachari, A. P. Rendell, J. C. Burant, S. S. Iyengar, J. Tomasi, M. Cossi, J. M. Millam, M. Klene, C. Adamo, R. Cammi, J. W. Ochterski, R. L. Martin, K. Morokuma, O. Farkas, J. B. Foresman, D. J. Fox, Gaussian 16, Revision C.01 Gaussian, Inc., Wallingford, CT, **2016**.
[25] T. Lu, F. Chen, *J. Comput. Chem.* **2012**, *33*, 580–592.
[26] C. I. Bayly, P. Cieplak, W. Cornell, P. A. Kollman, *J. Phys. Chem.* **1993**, *97*, 10269–10280.
[27] T. Lu, Sobtop, Version 1.0 (dev3.1), can be found under http://sobereva.com/soft/Sobtop, (accessed: 2023–01-01).
[28] J. Wang, R. M. Wolf, J. W. Caldwell, P. A. Kollman, D. A. Case, *J. Comput. Chem.* **2004**, *25*, 1157–1174.
[29] L. Martínez, R. Andrade, E. G. Birgin, J. M. Martínez, *J. Comput. Chem.* **2009**, *30*, 2157–2164.
[30] M. J. Abraham, T. Murtola, R. Schulz, S. Páll, J. C. Smith, B. Hess, E. Lindahl, *SoftwareX* **2015**, *1–2*, 19–25.
[31] W. Humphrey, A. Dalke, K. Schulten, *J. Mol. Graphics* **1996**, *14*, 33–38.
[32] Y. V. Mikhaylik, J. R. Akridge, *J. Electrochem. Soc.* **2004**, *151*, A1969-A1976.
[33] N. Tarantino, J. Y. Tinevez, E. F. Crowell, B. Boisson, R. Henriques, M. Mhlanga, F. Agou, A. Israël, E. Laplantine, *J. Cell Biol.* **2014**, *204*, 231–245.
[34] X. Michalet, *Phys. Rev. E* **2010**, *82*, 041914.
[35] E. D. North, R. R. White, *Ind. Eng. Chem.* **1951**, *43*, 2390–2397.

Manuscript received: December 3, 2023
Revised manuscript received: December 26, 2023
Version of record online: January 26, 2024

© 2024 Wiley-VCH GmbH

25666223, 2024, 4, Downloaded from https://chemistry-europe.onlinelibrary.wiley.com/doi/10.1002/batt.202300572 by University of Ulsan, Wiley Online Library on [11/11/2025]. See the Terms and Conditions (https://onlinelibrary.wiley.com/terms-and-conditions) on Wiley Online Library for rules of use; OA articles are governed by the applicable Creative Commons License